



Separation of saliency information for speed sensorless detection of induction machines flux and rotor position

Thomas M. Wolbank

*Department of Electrical Drives and Machines,
Vienna University of Technology, Vienna, Austria, and*

Mohamed K. Metwally

*Electrical Engineering Department, Faculty of Engineering,
Menoufiya University, Menoufiya, Egypt*

Abstract

Purpose – The purpose of this paper is to describe an effective method to eliminate or substantially reduce the modulation harmonics due to saturation and inter-modulation for sensorless speed control induction motor drives at low and zero speed with high loads using artificial neural networks (ANN).

Design/methodology/approach – In this paper, the separation of the saturation signal, the slotting signal, and the inter-modulation signal components in squirrel cage induction machines operating at low and zero frequency using ANN has been experimentally implemented and measurement results are given.

Findings – The measurement results show the advantages of the application of the proposed technique at low and zero speed sensorless control even at high load levels.

Originality/value – The paper describes an effective method of eliminating or reducing modulation harmonics in induction motor drives.

Keywords Control systems, Flux, Fourier transforms, Neural nets, Electric machines

Paper type Research paper

1. Introduction

For the highly dynamical behavior of the induction machine operated under any kind of field-oriented control (FOC), a position sensor (encoder) is needed. Research was placed on omitting this sensor using fundamental machine models but as the mathematical model utilizes the stator voltage equation it tends to deteriorate at low speed as result of a vanishing (back-emf). With an improved stator voltage measurement and integration these models can be improved in the lower frequency range but because of sensor errors and parameter variations those models are unable to guarantee long-term stability at zero fundamental frequency.

Thus, injection-based methods have been proposed as they are able to detect spatial saliencies of the induction machine. In this non-(fundamental wave)-model based sensorless control of AC machines the flux/rotor position can be determined by evaluating



the current response to voltage pulses. This current slope, in fact the first time derivative, is modulated by all spatial saliencies that are affecting the leakage inductance. The sources of these saliencies can be various, for instance the saturation of the machine by the main flux, the slotting, or lamination material anisotropy (Wolbank *et al.*, 2004). In case of the exploitation of the signal for control, only one of these spatial saliencies deals as the major effect, while the others have parasitic character.

A sensorless control scheme that works even in the critical range around zero would not only lead to a cheaper drive, but in addition also to an increased reliability as the shaft sensor and its cable is often the cause for a breakdown of the whole drive. To detect the necessary information of the rotor position or speed it is thus necessary to use non-fundamental effects in the machine.

Saliency tracking-based sensorless control methods have gained significant importance in combination with permanent magnet synchronous machines during the last years in applications where sustained sensorless operation in the low and zero speed range, and/or position control are needed, as they overcome the limitation of the methods based on the fundamental excitation (back-emf).

Different implementations of saliency tracking-based methods have been proposed, e.g. Jansen and Lorenz (1995), Cilia *et al.* (1997), Ha and Sul (1999), Consoli *et al.* (1999), Gao *et al.* (2007) and Schroedl (1996). While all of them share the same physical principles, significant differences between the methods exist. The differences are related to the high frequency excitation used, to the electrical signals that are measured to obtain information on the saliency position or to the algorithms used to track the saliency image. The method applied in this paper is the voltage pulse injection method, also denoted INFORM (Schroedl, 1996). All saliency tracking methods are affected by a flux/load dependence. Another point that has to be taken into account is that the saliency information of the flux (saturation dependent) is superposed with all other saliencies, present in an induction machine.

Different methods have been proposed in literature to reduce or eliminate the influence of load and flux level. They are usually based on filtering (Caruana *et al.*, 2002; Degner and Lorenz, 1997, 2000), function approximation or correction tables (Briz *et al.*, 2000), spatial filtering (Holtz and Pan, 2002), or the so-called space modulation profiling (Teske *et al.*, 2001). Compensation of saturation induced saliencies has usually been approached by means of lookup tables, which can be implemented in different ways (Briz *et al.*, 2004a, b; Holtz and Pan, 2004; Teske *et al.*, 2000). In all of them, the table is built during an off-line commissioning process for different operating points of the machine. The lookup table is then accessed during the regular sensorless operation of the drive, and its information used for on-line decoupling of the saturation induced components of the measured signals. Using a lookup table for decoupling of saturation-induced components has some limitations. The amount of information that needs to be stored in the lookup table is unknown and it is not obvious how to determine either the range of operating conditions needed for each of them (Garcia *et al.*, 2005). Compensation of inter-modulation induced saliencies has usually been approached using side band filter (Gao *et al.*, 2007), or the so-called structure neural network (SNN) (Garcia *et al.*, 2005). The SNN organizes the layers of the network according to the expression of the zero sequence carrier voltage in the synchronous frame, with each layer representing some terms of the expression, and the SNN is only trained under limited load conditions.

Calculating these dependencies will consume some amount of calculation power as well as an exact error description of the system influences in all points of operation, which can only be performed by experts and which can be very time consuming.

In the following, separation of the saturation, the slotting signals and the inter-modulation signals components in squirrel cage induction machine operating at low and zero frequency using artificial neural networks (ANN) has been experimentally implemented, measurement results are given to show the advantages of the application of the proposed technique to low and zero speed sensorless control even at high load levels.

2. Main saliencies in the transient current response signal

As already mentioned the sensorless speed and position estimation is achieved by injection of additional transient excitation voltage pulses to the machine (Schroedl, 1996). It is based on spatial differences in the leakage inductance and utilizes these differences by evaluating the response of the machine due to the transient excitation. This excitation is generated with the inverter by applying short voltage pulses.

Assuming zero electrical frequency the back electromotive force of the fundamental wave is zero. Then a voltage pulse leads to a transient change of the armature current. This current change can be expressed as a current change phasor, which should point in the same direction as the voltage phasor of the applied voltage pulse. Owing to non-fundamental wave effects in the machine there is a deviation from this alignment detectable. By applying an algorithm to the measured current change phasor, the influence of the (back-emf) can be eliminated and the signal obtained is modulated with these non-fundamental effects only.

However, the main problem in sensorless control currently is not the detection of these saliencies but their reliable separation in all operating states as all of them are contained in one resulting control signal. Generally, there are three main saliencies present in standard induction machines as shown in Figure 1. There is the saturation saliency, which is caused by the different levels of saturation of the machine lamination along the circumference. It is usually the most prominent modulation especially when the machine is loaded. Its main signal component has twice the electrical frequency of the fundamental wave as only the saturation level not its direction is detected. Its spatial angle is thus dependent on both the directions of the main flux and that of the leakage flux of the machine. The slotting saliency is caused by the slotting of the stator and rotor lamination. It has a main signal component in the resulting signal that is rotating with the mechanical speed times the number of rotor slots. Its magnitude ranges from negligible in machines with closed rotor slots to about the

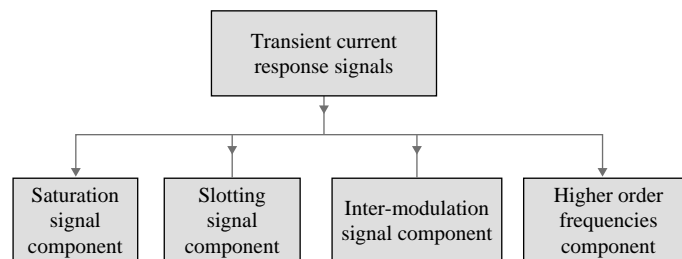


Figure 1.
Structure of saliencies
component in transient
current response signal

same order of magnitude as the saturation saliency in un-skewed open slot machines. Generally, there is also a signal component detectable with a period that equals the number of rotor slots + or - the harmonic number of the saturation. This inter-modulation component, as the saturation saliency, also depends on the saturation level. There is finally also a third saliency not measured or isolated (separated) in the measurements of standard induction machines. It has so far not been considered for the control of induction machines. It is caused by the lamination material anisotropy and has a period of two along the rotor surface according to the crystalline anisotropy of iron.

In the resulting control signal all signal components of the mentioned main saliencies as well as their inter-modulations are present and superposed. It is obvious that there are specific operating conditions where for example the frequency of the saturation component equals that of the main slotting component (fundamental frequency equals mechanical speed times number of rotor slots). In these cases an exact separation of the two components is not possible in practical operation.

3. Artificial neural network

The separation process for the saturation and inter-modulation saliencies is done using ANN. A number of methods have been developed for ANN learning. Learning methods may be either supervised, or unsupervised. Supervised learning is required for pattern matching. The back-propagation network is the most popular of the supervised learning techniques (Haykin, 1998; Wolbank *et al.*, 2007). Its advantages include high learning accuracy, high recall speed, etc. The structure of the neural network used in this paper, a Multi Layer Perceptron is shown in Figure 2. Two neurons are used

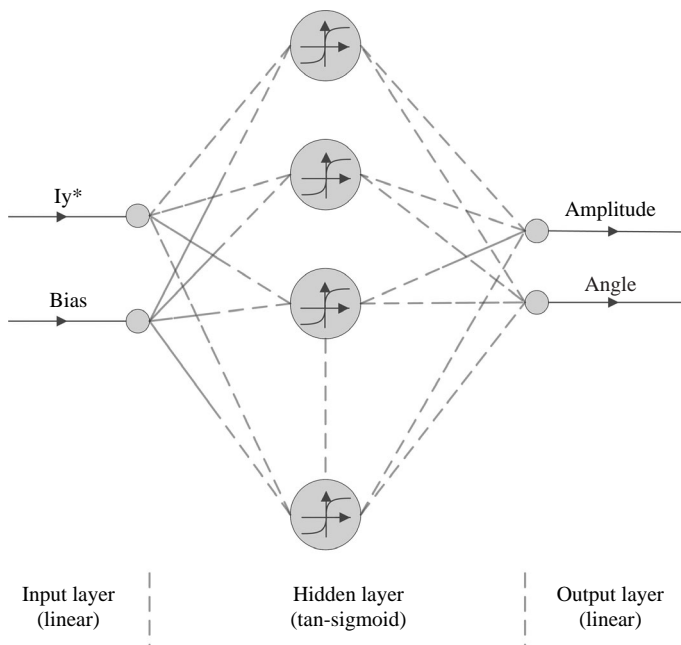


Figure 2.
Structure of neural network

in the input-layer, five in the hidden-layer and two neurons in the output-layer. The input to the ANN is the load current and the outputs are the amplitude and angle of the compensated disturbance signal of the saturation saliency component.

The ANN had been trained using the amplitudes and angles of the saturation disturbance signal obtained from fast Fourier transform (FFT) analysis of the saliency signal shown in Figure 3 at different loads as targets. After the training phase the ANN interpolates to get the amplitudes and angles at all load conditions. The training phase had been done offline on a separated system programmable under MATLAB/Simulink and the resulting input and output weights of the training phase are then used for the online phase of ANN. The same procedure is done but with the amplitude and angle of the inter-modulation saliency to reduce the inter-modulation saliency signal. Using the outputs of the neural network the main component related to the saturation saliency can be almost totally removed and the inter-modulation slotting saliency can be clearly reduced as shown in Figure 4 middle and lower diagrams, respectively.

4. Separation of rotor slotting and saturation saliencies

Figure 5 shows the structure of saliency signal separation scheme using the proposed compensation algorithm and the identification method for extraction of the slotting by eliminating saturation and inter-modulation saliencies disturbances with a rotor position estimator. The remaining signal component is the slotting signal that is superposed with a high frequency component that can be removed using low pass filter (LPF). The outputs from ANN are the amplitudes and compensated angles of saturation and inter-modulation saliencies, respectively.

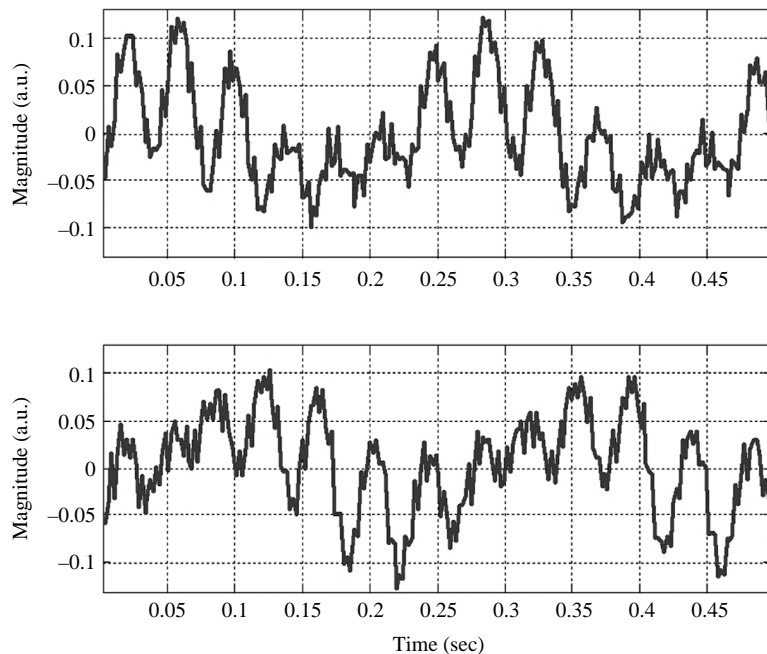
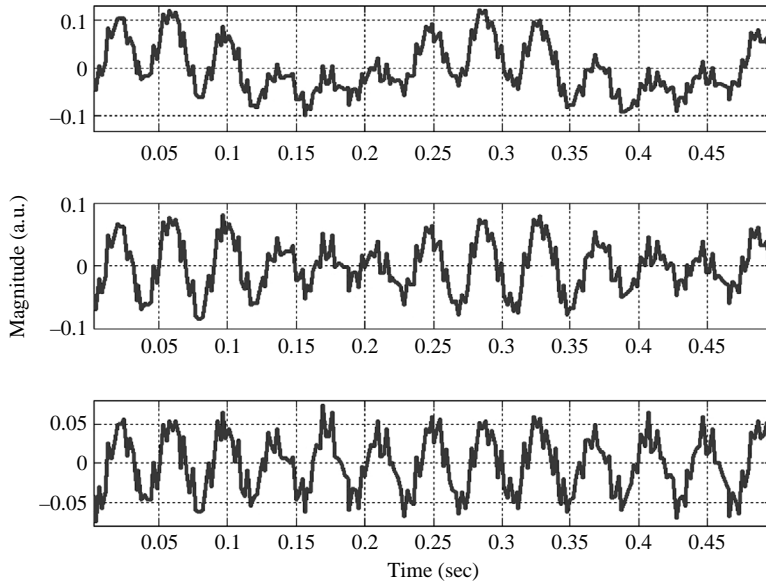


Figure 3.
Real and imaginary part of
saliency control signal
during one electrical
revolution at 90 per cent
rated load



Notes: Upper: no compensation; middle: compensation of saturation; lower: compensation of saturation and inter-modulation saliencies

Figure 4. Real component of position control signal at 90 per cent rated load

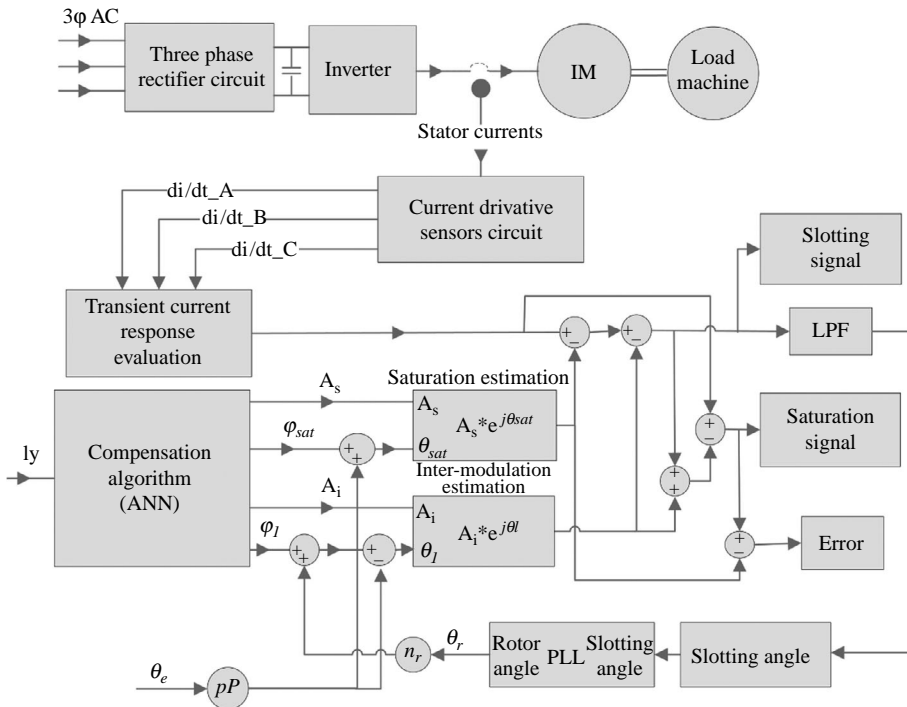


Figure 5. Structure of saliency signal separation with rotor position estimator

These parameters are dependent on the load and flux level of the machine. The rotating angles for elimination of saturation and reduction of inter-modulation saliencies are given in equations (1)-(2):

$$\theta_{sat} = p\theta_e + \varphi_{sat} \quad (1)$$

$$\theta_I = n_r\theta_r^\circ - p\theta_e + \varphi_I \quad (2)$$

Where θ_e is the stator current angle, θ_r° is the estimated rotor angle, φ_{sat} the saturation compensated angle, φ_I the inter-modulation compensation angle, p is number of poles pair, and n_r is number of rotor slots, respectively. By using the (sine, cosine) functions of these angles with the two amplitudes (A_s , A_i shown in Figure 5) for saturation, inter-modulation signals, respectively, and subtracting the resulting signals from the saliency control signal the saturation saliency component can be almost totally removed and the inter-modulation saliency component can be clearly reduced as shown in Figure 4 middle and lower diagrams, respectively.

Figure 6 shows the FFT spectrum of the saliency control signal before compensation (upper diagram), and after compensation of saturation and inter-modulation signals (lower diagram). The output signal from LPF is the control signal with only the slotting frequency as a dominant signal. Using the harmonic compensation scheme as in Figure 2 is preferably applied, when the saliency to be exploited for control is the slotting.

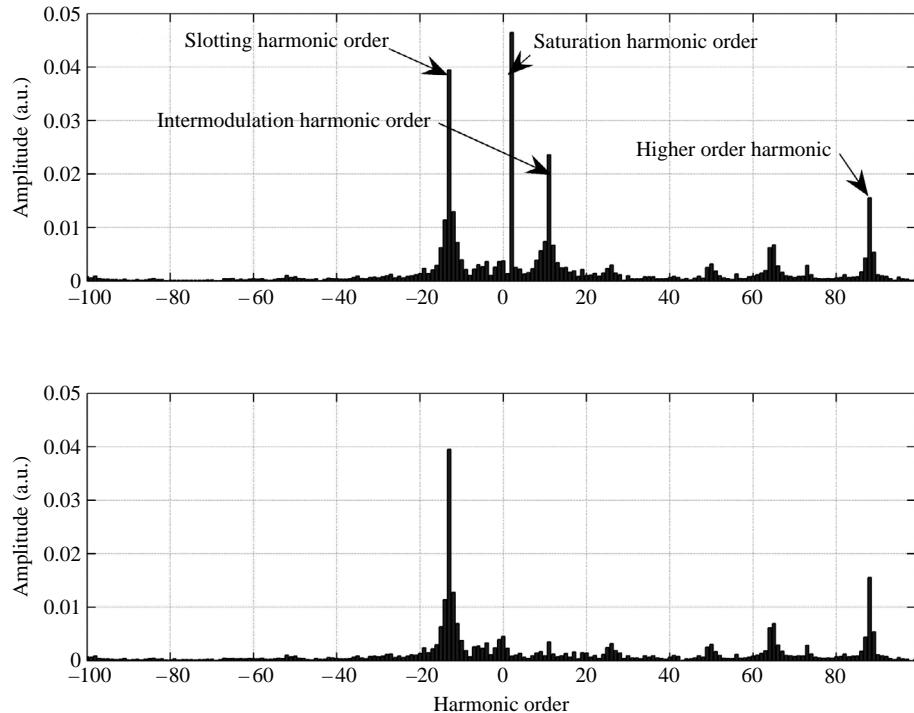


Figure 6.
FFT spectrum of saliency
signal at 90 per cent rated
load

Notes: Upper: no compensation; lower: compensation of saturation and inter-modulation

Subtracting the extracted slotting signals together with inter-modulation signal from the main saliency signal leads to the saturation signal. Comparing this saturation signal with the saturation signal output from ANN an indicator for the efficiency of the compensation algorithm is obtained denoted “error” in Figure 5.

The slotting signal is used in combination with a phase locked loop to detect the estimated rotor position angle. This estimated angle (θ_r) is also used to compensate the inter-modulation effect as shown in Figure 5. The estimated rotor position can be combined with the current model (rotor equation) to get the estimated flux angle used for FOC and the saturation signal can be used for stabilizing the flux angle estimation using the stator voltage model (stator equation). This investigation is focused on signal processing to establish a reliable separation of the saliencies.

The flux calculation in (FOC) using fundamental wave models in combination with the saliency signals is thus out of the scope of this paper. Detailed description on this topic can be found for example in Holtz (1996).

5. Experimental results

The experimental results shown are obtained from an induction machine drive coupled to a speed controlled load dynamometer as a load shown in Figure 5. The machine under test was operated under field-oriented torque controlled conditions using the compensation scheme for saturation and inter-modulation saliencies. The speed is determined by a load dynamometer under speed controlled mode. The parameters of the induction motor are given in the Appendix. The control is done on an industrial digital signal processor board plugged into a computer. It performs the vector control algorithm and compensation scheme using ANN. The pulse sequences and instances of injections of the pulses are being calculated on a field programmable gate array system plugged into another computer. There is a communication board between the two systems for transferring and receiving data between them. The induction motor was fed by a voltage source inverter and three current sensors were used for the current measurements. An optional position signal is available from an optical encoder with 1,024 pulses per revolution used as a reference signal. The proposed technique has been programmed and experimentally implemented with the voltage pulse injection method on the induction machine at different load and speed levels. The resulting performance of the proposed technique can be seen in the following figures.

Figure 3 shows the saliency signals of the transient current response during one electrical revolution (13 slotting periods) at 90 per cent rated load, rated flux and speed 34 rpm.

Figure 6 (upper diagram) shows the FFT spectrum of the transient current response signal during one electrical revolution. As noted from Figure 6, the FFT spectrum contains the components of the slotting, the saturation, the inter-modulation and higher order harmonics superposed to each other.

In order to track the slotting component, the other components should be eliminated or reduced as described before, using the ANN. As noted from Figure 4 (lower diagram), the remaining signal after the compensation only contains the slotting component as a dominant saliency component and higher order harmonics.

Figure 6 (lower diagram) shows the FFT spectrum of the remaining signal after elimination of the disturbance components. The saturation saliency is removed

and the inter-modulation saliency amplitude is decreased. The remaining signal still shows some higher frequency disturbances which are then filtered using LPF.

Figure 7 (upper diagram) shows the real part of the estimated saturation signal during one electrical revolution. The machine has been operated with 90 per cent rated load, rated flux and a speed of 34 rpm. The separated electrical angle (black) and the slotting angle (red) during one electrical revolution are given in the lower diagram of Figure 7, which confirms the efficiency of the tracking algorithm. When comparing Figures 5 and 7 it can be noted that the slotting angle and the saturation angle (= twice the flux angle) are rotating in opposite directions in the FFT spectrum as well as in the separated signal traces. This effect is a result of the number of slots in the stator (36) and rotor (44).

Figure 8 gives a picture showing the quality of the tracking algorithm for rotor slots by using a slot counter. Each revolution of the estimated slotting angle will increase the slot counter by one. For comparison and grading a second counter is derived from the mechanical rotor angle obtained with a position encoder (44 slots per 2π). The counters are set to zero each time the value reaches 250.

Figure 8 shows the output of the counter during a speed change from 15.7 to 39.8 rpm with 90 per cent rated load. As shown in the figure, the output of the counter of the actual rotor slots (black) and counter for the estimated rotor slots (red) is exactly the same which confirms the high accuracy of the separation algorithm allowing a precise detection of the rotor position even at high load levels.

The phase difference between the estimated and reference position visible in the figure results from a non-zero position offset. The slotting signal only delivers

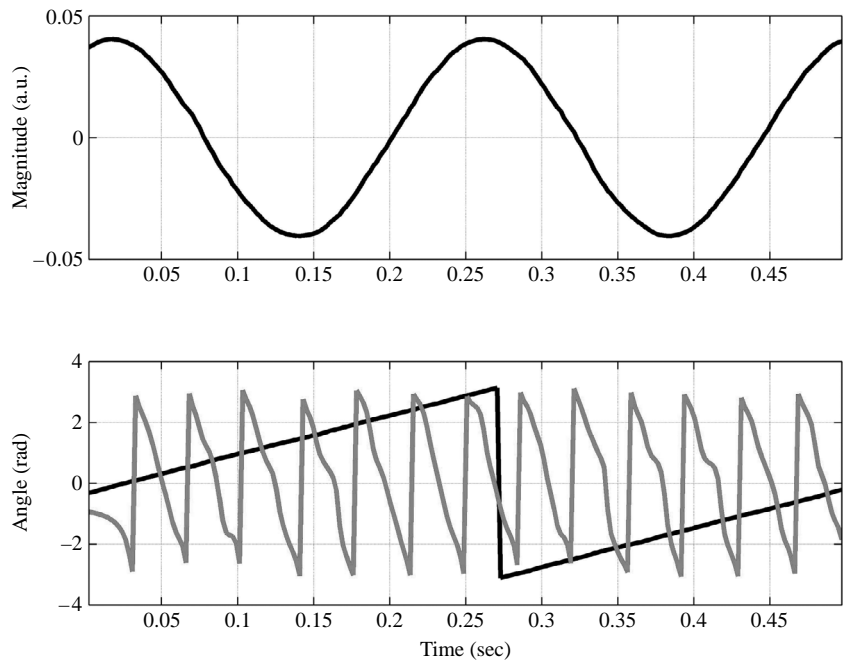


Figure 7.
Upper: real component of the separated saturation saliency signal and lower: electrical angle (black), slotting angle (red)

Note: Load current: 90 per cent rated

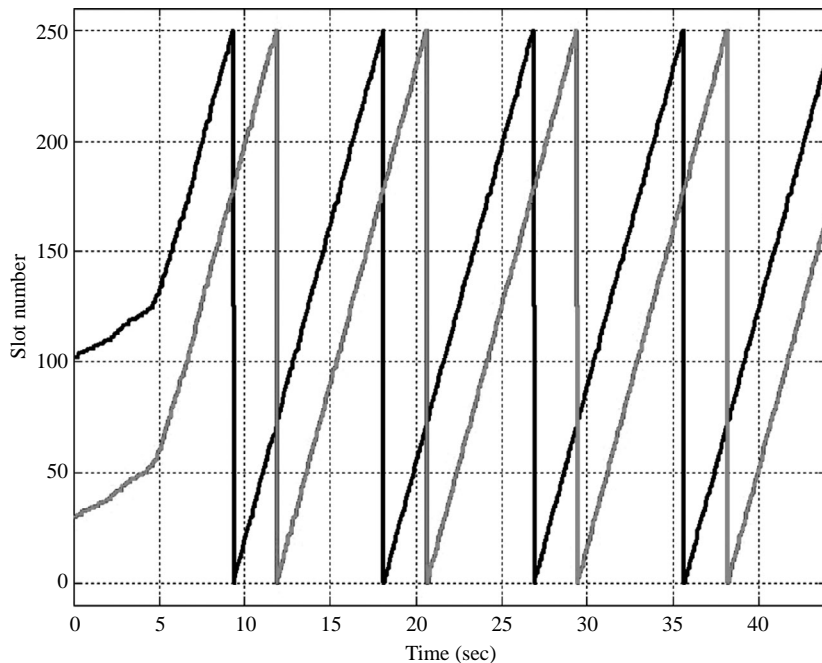


Figure 8. Slotting counter values during speed up from 7.7 to 39.8 rpm with 90 per cent rated load using mechanical sensor (black); using separated slotting modulation (red)

incremental information on the mechanical angle thus no absolute position can be obtained. The quality of estimated position signal and the constant position offset is clearly seen.

Figure 9 shows the slotting counter with the machine running at zero speed and at no load condition for the first 8 s then the load is increased stepwise from 0 to 90 per cent rated load at time instant approximately equal $t = 8$ s and back from 90 to 0 per cent at $t = 49$ s, respectively, in a ramp function. The reason for using a ramp instead of a step is not a dynamic limitation of the proposed method itself, but is caused by the measurement system used (dynamic of speed controlled dynamometer and sampling rate of the current derivative measurement). During a big transient load step the slotting frequency would be increased for a short period above the Shannon frequency impressed by the sampling rate of the measurement system (~ 200 Hz).

It can be seen in the figure that as long as the Shannon condition is met the offset between the two slotting counters stays constant during the whole period independent from the load and even during the sudden load changes when the magnitudes of the saturation and inter-modulation components also change very distinctly.

6. Conclusion

This paper has described an effective method to eliminate or substantially reduce the modulation harmonics due to saturation and inter-modulation for sensorless speed control induction motor drives at low and zero speed with high loads using ANN. These harmonics effects arise due to load or flux level changes. An accurate and reliable compensation algorithm for the saturation and inter-modulation disturbance effects has been presented. The performance of the separation algorithm for the slotting signal has

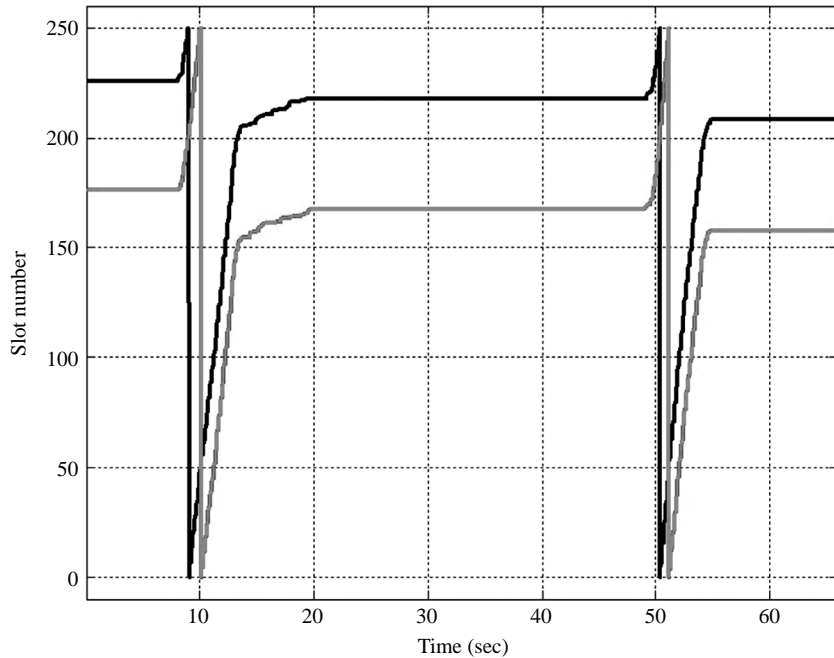


Figure 9.
Slotting counter values during sudden load change at zero speed, mechanical sensor based (black); using separated slotting modulation (red)

Note: Load current changed from 0 to 90 per cent rated load at $t = 8$; back to 0 at $t = 49$

been tested and verified using counter for the slotting signal compared with actual slotting signal from the mechanical angle at low and zero speed tests with high load levels.

References

- Briz, F., Denger, M.W., Diez, A. and Lorenz, R.D. (2000), "Measuring, modeling and decoupling of saturation-induced saliencies in carrier signal injection based sensorless AC drives", *Proceedings of IEEE Industry Applications Conference*, Vol. 3, pp. 1842-9.
- Briz, F., Degner, M.W., Garcia, P. and Guerrero, J.M. (2004a), "Rotor position estimation of AC machines using the zero sequence carrier signal voltage", *Proceedings of the IEEE-IAS Annual Meeting, Seattle, WA, USA, October*, pp. 1305-12.
- Briz, F., Degner, M.W., Garcia, P. and Lorenz, R.D. (2004b), "Comparison of saliency-based sensorless control techniques for AC machines", *IEEE Trans. on Ind. Appl.*, Vol. 40 No. 4, pp. 1107-15.
- Caruana, C., Asher, G.M., Bradley, K.J. and Woolfson, M. (2002), "Flux position estimation in cage induction machines using synchronous H_f injection and Kalman filtering", *Proceeding of IEEE Industry Application Annual Meeting*, Vol. 2, pp. 845-50.
- Cilia, J., Asher, G.M. and Bradley, K.J. (1997), "Sensorless position detection for vector controlled induction motor drives using an asymmetric outer section cage", *IEEE Trans. on Ind. Appl.*, Vol. 33, pp. 1162-9.
- Consoli, A., Scarcella, G. and Testa, A. (1999), "A new zero frequency flux position detection approach for direct field oriented control drives", *Proceedings of the IEEE-IAS Annual Meeting, Phoenix, AZ, USA*, Vol. 4, pp. 2290-7.

-
- Degner, M.W. and Lorenz, R.D. (1997), "Using multiple saliencies for the estimation of flux, position, and velocity in AC machines", *Proceedings of IEEE IAS Annual Meeting, New Orleans, LA, USA*, pp. 760-7.
- Degner, M.W. and Lorenz, R.D. (2000), "Position estimation in induction machines utilizing rotor bar slot harmonics and carrier frequency signal injection", *IEEE Trans. on Ind. Appl.*, Vol. 36 No. 3, pp. 736-42.
- Gao, Q., Asher, G.M. and Sumner, M. (2007), "Sensorless position and speed control of induction motors using high frequency injection and without offline precommissioning", *IEEE Trans. on Industrial Electronics*, Vol. 54, pp. 2474-81.
- Garcia, P., Briz, F., Racn, D. and Lorenz, R.D. (2005), "Saliency tracking-based sensorless control of AC machines using structured neural networks", *Proceedings of IEEE Industry Applications Annual Meeting, IAS, New Orleans, LA, USA*.
- Ha, J. and Sul, S. (1999), "Sensorless field-orientation control of an induction machine by high frequency signal injection", *IEEE Trans. on Ind. Appl.*, Vol. 35 No. 1, pp. 45-51.
- Haykin, S.S. (1998), *Neural Networks: A Comprehensive Foundation*, 2nd ed., Prentice-Hall, Englewood Cliffs, NJ.
- Holtz, J. (1996), "Methods for speed sensorless control of AC drives", in Rajashekara, K. (Ed.), *Sensorless Control of AC Motor Drives*, IEEE Press Book, New York, NY.
- Holtz, J. and Pan, H. (2002), "Elimination of saturation effects in sensorless position controlled induction motors", *Proceedings of IEEE Industry Applications Annual Meeting, New Orleans, LA, USA*, Vol. 3, pp. 1695-702.
- Holtz, J. and Pan, H. (2004), "Elimination of saturation effects in sensorless position-controlled induction motors", *IEEE Trans. on Ind. Appl.*, Vol. 40 No. 2, pp. 623-31.
- Jansen, P.L. and Lorenz, R.D. (1995), "Transducerless position and velocity estimation in induction and salient AC machines", *IEEE Trans. on Ind. Appl.*, Vol. 31, pp. 240-7.
- Schroedl, M. (1996), "Sensorless control of AC machines at low speed and standstill based on the INFORM method", *Proceedings of 31st IAS Annual Meeting, San Diego, CA, USA*, Vol. 1, pp. 270-7.
- Teske, N., Asher, G.M., Sumner, M. and Bradley, K.J. (2000), "Suppression of saturation saliency effects for the sensorless position control of induction motor drives under loaded conditions", *IEEE Trans. on Industrial Electronics*, Vol. 47, pp. 1142-50.
- Teske, N., Asher, G.M., Sumner, M. and Bradley, K.J. (2001), "Encoderless position estimation for symmetric cage induction machines under loaded conditions", *IEEE Trans. on Ind. Appl.*, Vol. 37 No. 6, pp. 1793-800.
- Wolbank, Th.M., Machl, J.L. and Hauser, H. (2004), "Separating anisotropic material effects in the control signals of inverter-fed AC machines", *Journal of Magnetism and Magnetic Materials*, Vols 272-276, pp. E1701-3 (supplement 1).
- Wolbank, Th.M., Vogelsberger, M.A. and Stumberger, R.H. (2007), "Adaptive flux model for commissioning of signal injection based zero speed sensorless flux control of induction machines", *IEEE International Conference on Power Electronic and Drive Systems (PEDS)*, pp. 1157-62.

Appendix

Machine parameters of the applied induction machine:

Nominal current: 30 A.

Nominal voltage: 280 V.

COMPEL
29,5

Nominal frequency: 75 Hz.
Rated power: 11 kW.
four-poles, 36 stator teeth, 44 un-skewed rotor bars.

1392

About the authors



Thomas M. Wolbank, studied Industrial Electronics at the Vienna University of Technology in Austria where he also received the Doctor degree in 1996 and the Ao. Univ.-Prof. Degree in 2004, respectively. At present he is with the Department of Electrical Drives and Machines at the Vienna University of Technology (web site: www.tuwien.ac.at). Thomas M. Wolbank is the corresponding author and can be contacted at: thomas.wolbank@tuwien.ac.at



Mohamed K. Metwally, received the BSc with honor and MSc degrees in Electrical Engineering from the Menoufiya University, Egypt, in 1999 and 2003, respectively, and the PhD degree with distinction from the Vienna University of Technology, Austria in 2009. He is currently a Lecturer in Electrical Engineering Department, Menoufiya University, Egypt.